ORIENTAL JOURNAL OF CHEMISTRY
An International Open Access, Peer Reviewed Research Journal
www.orientjchem.org
ISSN: 0970-020 X
CODEN: OJCHEG
2026, Vol. 42, No.(2):
Pg. 567-575

Supramolecular Assembly of β-Caryophyllene β- Cyclodextrin Complex-Spectral Approach

SK. DEVI and J. PREMA KUMARI*

Department of Chemistry, Scott Christian College (Autonomous), Nagercoil-629003.
Affiliated to Manonmaniam Sundaranar University, Tirunelveli.
*Corresponding author E-mail: premaisaac67@gmail.com

http://dx.doi.org/10.13005/ojc/420218

(Received: June 14, 2025; Accepted: January 22, 2026)

ABSTRACT

Beta-Caryophyllene (BCP) is a naturally occurring sesquiterpene with a variety of biological functions; however, its low water solubility limits its therapeutic application. In this study, BCP was extracted from *Aegle marmelos* leaves using column chromatography. To enhance its solubility and bioavailability, BCP was encapsulated in β-Cyclodextrin (β-CD). A solid inclusion complex was formed and characterized using FT-IR, ^{1}H-NMR, thermal analysis, and SEM imaging. A liquid inclusion complex was also prepared and evaluated through absorbance and emission spectrum analysis. Molecular docking revealed a stable interaction between BCP and β-CD, indicating improved encapsulation efficiency. Furthermore, an anti-diabetic and anti-inflammation assay was performed to assess the therapeutic efficacy of the inclusion complex. These findings suggest that using ββ-CD as a carrier system can enhance the physiological effects and medical applications of BCP.

Key words: BCP:ββCD, TG-DTA, Molecular docking, Phase Solubility, Anti-inflammation, Anti-diabetic.

INTRODUCITON

Medicinal plants are crucial to India's prehistoric medical system. Pharmacological studies have recognized the worth of medicinal plants as a source of pharmacological agents.[1] Herbal medicine is well-known out there, the methods employed for millennia to treat basic ailments such as colds and gastrointestinal disorders. Its renown continues to grow.[2] *Aegle marmelos* (L.) is important medicinal plant available in Tamilnadu, India and are reported to have various medicinal property in Traditional medical systems.[3]Beta-caryophyllene (BCP) is a desire sesquiterpene with a wide range of applications, including medicines, flavorings, and fragrances.[4] This chemical is very volatile, poorly water soluble, and sensitive to light, oxygen, humidity, and high temperatures.[5] Over a century ago, Schardinger

discovered cyclic oligosaccharides (CDs), a type of carbohydrate.[6] ββ-CD is a promising drug delivery material due to its low biotoxicity and good biocompatibility.[5] Since 1998, ββ-cyclodextrin, a 2% flavor carrier and food protectant, has been GRAS-listed. The research focuses on the encapsulation of sterilizing chemicals.[7] CDs are utilized in the food, pharmaceutical, and environmental sectors.[8] The primary feature of cyclodextrins is their capacity to use molecular complexation to create solid inclusion complexes, also known as host–guest complexes, with a wide variety of solid, liquid, and gaseous substances.[9] In silico modeling is a beneficial technique in deciding active bio-molecules among illicit drugs with pharmacological potential.[10]

This study intends to synthesize and characterize the solid inclusion complex of BCP with ββ-CD to boost its solubility, stability, and biological activity. The inclusion complex is examined spectroscopically to ensure encapsulation. Phase solubility for the included compound is tested for BCP with different concentrations of ββ-CD. Besides, molecular docking was conducted to investigate the interaction of binding stability and anti-inflammatory activity was tested to find bioactivity of BCP within the β-CD cavity.

MATERIALS AND METHODS

Preparation of compound

After being collected at Derisanamcope, Kanyakumari, the leaves of *Aegle marmelos* were cleaned, dried, and ground into a fine powder. Ethanol was used as a solvent in the extraction process utilizing the Soxhlet method. column chromatography was used to isolate the BCP component.

Preparation of solid inclusion complex

With a normalcy of 0.01 N, 0.340 g of β-CD and 0.0612 g of BCP are dissolved in 30 ml of double-distilled water and 30 ml of ethanol, respectively. Both solvents are continuously stirred for 48 hours. The solid inclusion complex is then produced by filtering and drying the product. FT-IR analysis was carried out from ANJAC, Shimadzu FT-IR Spectrometer, Sivakasi. ^{1}H-NMR from Spectroscopy is performed using Bruker Avance 400 MHz, Gandhigram Rural University. STA from Manonmanium Sundaranar University, Tirunelveli is used to conducting TG-DTA analysis. SEM testing from Manonmanium Sundaranar University, Tirunelveli, were tested to confirm the formation inclusion compound.

Preparation of liquid inclusion complexes

0.0681 g of β-CD was dissolved in 30 ml of double-distilled water, and 0.0040 g of BCP was dissolved in 10 ml of ethanol to create a solution of the chemical. In order to create liquid inclusion complexes, the β-CD concentration was methodically changed. Both fluorescence and UV-Vis spectroscopy were used to examine the resultant compounds. A Systronics Double Beam Spectrophotometer-2203 was used to record the UV-Vis absorption spectra, and a JASCO Spectrofluorometer FP-8200 was used to get the fluorescence emission spectra of the inclusion complexes. Scott Christian College in Nagercoil was the site of both spectroscopic analyses.

Phase Solubility

Solutions with different concentrations of β-CD were generated and examined in order to assess the solubility of BCP in the presence of β-CD. 0.340 g of βCD was individually dissolved in 30ml of double-distilled water, and 0.0204 g of BCP was dissolved in 10ml of ethanol to create a stock solution. To guarantee appropriate interaction and possible inclusion complex formation, the produced β-CD solutions were gradually combined with BCP and shook constantly for 72 hours. A Systronics Double Beam Spectrophotometer-2203 was used for the UV-Vis spectrum analysis, and all measurements were made at Scott Christian College in Nagercoil.

Molecular Docking

The PubChem database provided the BCP three-dimensional structural data in SDF format. After that, AutoDock software was used to convert this structure into PDB format so that docking simulations could use it. Likewise, ββ-CD's 3D structural information was obtained from the ChemSpider database. The AutoDock Vina server was used to conduct the molecular docking study, with ββ-CD serving as the receptor and BCP as the ligand. This computational approach permitted the insertion of the BCP molecule within the βCD cavity, permitting the study of their binding interactions and complex formation.

Anti-Inflammatory Potential

Blood from a healthy volunteer was processed to obtain a 10% RBC suspension. Test samples (100–500 µg/mL) were mixed with RBCs and incubated at 56°C for 30 minutes. After cooling and centrifugation, absorbance of the supernatant was measured at 560 nm.[16,17]

Anti-Diabetic Activity

Samples (50–600 µg/ml) and acarbose (50 µg/ml) were incubated with βamylase in phosphate buffer (pH 6.9) at 25°C. After adding starch, the reaction was stopped with DNSA, boiled, and absorbance was measured at 540 nm. Inhibition (%) was calculated from triplicate tests[18,19].

RESULT AND DISCUSSION

Column Chromatography

Ethyl acetate and hexane in a 20:80 ratio were used as the mobile phase in column chromatography to purify and isolate the target chemical. TLC was carried out on a chosen fraction to validate the presence of the desired compound, and UV-Vis spectrum was used to confirm it. Fig. 1. shows the UV-Vis spectrum of BCP compound, further confirming that it was successfully identified and separated.

FT-IR Spectral Analysis

Fig. 2(a), 2(b), and 2(c) display the FT-IR spectral analysis of BCP, ββ-CD, and their solid inclusion complex. The development of the BCP:ββ-CD inclusion complex is confirmed by the vibrational frequency alterations that have been observed. While the CHβbending vibration of BCP, which was initially at 2924.10 cm^{-1}, shifts to 1383.83 cm^{-1}, the C-H stretching vibration of BCP shifts to 2930.42 cm^{-1}. Likewise, encapsulation-induced alterations are indicated by the C=C stretching vibration at 1625.69 cm^{-1} shifting to 1629.02 cm^{-1}. At 3434.25 cm^{-1}, the O-H stretching vibration moves to 3436.86 cm^{-1} for β-CD, indicating hydrogen bonding with BCP. Confirming host-guest interactions, the C-H

Table 1: 1H-NMR Spectrum of BCP:β-CD Inclusion complex

Proton	β-CD (ppm)	BCP:ββ-CD(ppm)	Δδ
H1	4.998	4.978	0.020
H2	3.573	3.566	0.007
H3	3.873	3.835	0.038
H4	-	-	-
H5	3.538	3.508	0.030
H6	-	-	-

Table 2: Absorption of BCP with β-CD at different concentration

Concentration of β-CD	λ_{max}	Absorbance
0	205	1.417
0.002	206.2	1.816
0.004	207.6	2.002
0.006	208	2.418
0.008	208.4	2.700
0.01	209	3.762

Table 3: Fluorescence Emission of BCP withβ-CD at different concentration

Concentration of β-CD	λ_{max}	Intensity
0	300.8	260
0.002	305.2	265
0.004	310	268.4
0.006	317.2	272
0.008	326.8	273.8
0.01	334	280

Table 4: Auto dock vina results of BCP with β-CD

Mode (kcal/mol)	Affinity from	Dist from Rmsd L.B	Dist from Rmsd U.B
1	-4.952	0	0
2	-4.937	1.093	3.232
3	-4.912	1.596	3.757
4	-4.883	1.171	3.699
5	-4.791	1.428	4.002
6	-4.653	1.506	3.271
7	-4.643	0.98	3.999
8	-4.447	1.653	3.24
9	-4.417	1.674	3.111

Table 5: βα-Amylase Inhibition by BCP: β-CD at Various Concentrations

S.No	Concentration	OD I	OD II
1.	Untreated	1.57	1.59
2.	Acarbose	0.03	0.03
3.	50 µg/mL	1.22	1.21
4.	100 µg/mL	1.05	1.06
5.	200 µg/mL	0.87	0.88
6.	400 µg/mL	0.68	0.67
7.	600 µg/mL	0.56	0.57

IC50 : 31.35

stretching at 1462.31 cm^{-1} moves to 1454.26 cm^{-1} and the C-O-C stretching at 1109.89 cm^{-1} moves to 1126.62 cm^{-1}. The shift changes in the FT-IR spectra of ββ-CD, BCP, and their inclusion complexes show that the host β-CD and the guest compound BCP are included.

Table 1 and Fig.3(a), Fig.3(b) illustrate the interactions between the host (β-CD) and the guest (BCP). The H3 and H5 protons of ββ-CD are located within the inner cavity, while H1 and H2 protons are positioned near the outer surface of the cyclodextrin rim. Notably, in the ^{1}H-NMR spectrum of the inclusion complex, the signals corresponding to the H4 and H6 protons are not observed. This absence may be attributed to the deep inclusion of the BCP molecule within the β-CD cavity, which alters the local magnetic environment and potentially causes signal broadening or shifting beyond the detectable range. The changes observed for the internal cavity protons (H3 and H5), along with the disappearance of H4 and H6 signals, support the successful encapsulation of the BCP guest within the β-CD host cavity.

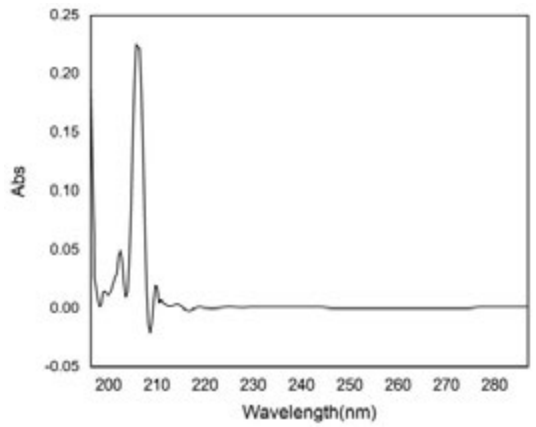

Fig.1. UV-Vis spectrum of BCP compound

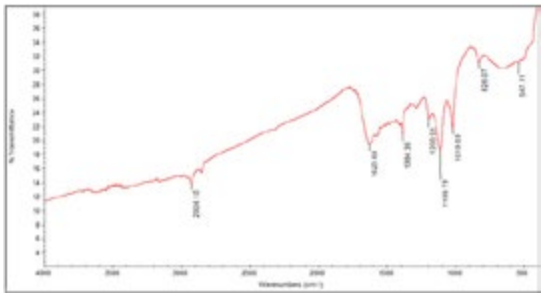

Fig. 2(a). FT-IR Spectrum of BCP

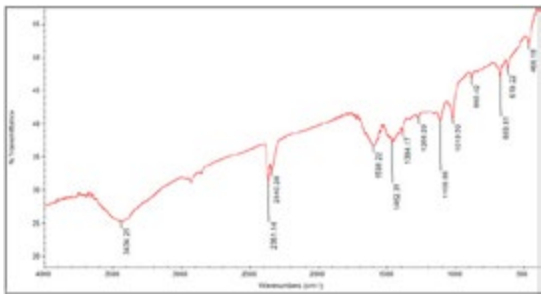

Fig. 2(b). FT-IR Spectrum of β-CD

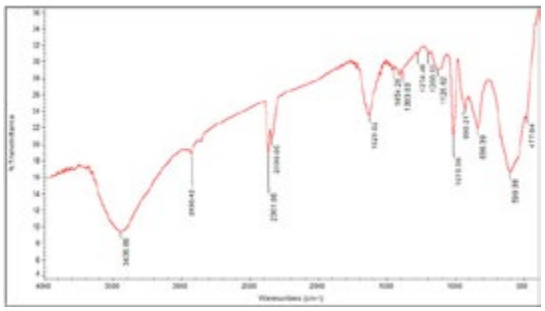

Fig.2(c). FT-IR Spectrum of BCP:β-CD Inclusion complex

The successful formation of the inclusion complex is supported by the SEM images. **Fig. 4(a)** displays the BCP guest as a porous, sponge-like aggregated structure, while **Fig.4(b)** shows the βCD host with a flaky and irregular morphology. Upon complexation, **Fig. 4(c)** reveals a distinct morphological transformation into a more uniform and crystalline structure, indicative of a stable inclusion complex. This notable change in surface morphology

reflects improved structural homogeneity, further confirming the effective encapsulation of BCP within the βCD cavity.

Phase Solubility

Fig.5 shows the relationship between the concentrations of BCP and β-CD in the aqueous solution is depicted in the phase solubility. The creation of a 1:1 inclusion complex is indicated by the graph and the stability constant value is 125M^{-1}, which shows a linear increase in BCP concentration with increasing β-CD concentration. The plot's linearity points to an A_L-type phase solubility profile, indicating that in the presence of β-CD, a soluble complex with increased BCP solubility forms.

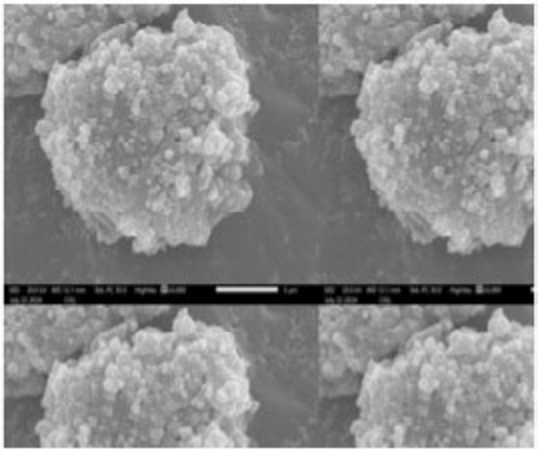

Fig. 4(a). SEM analysis BCP

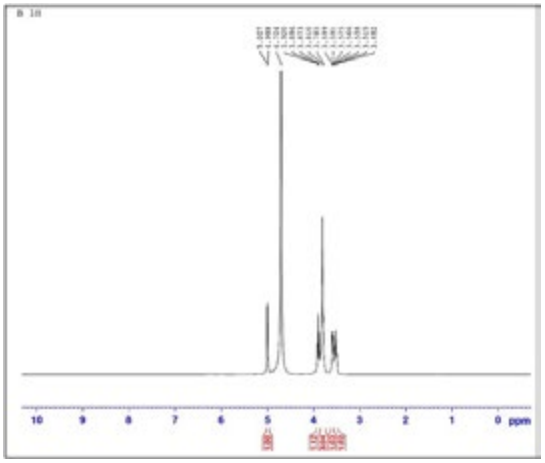

Fig. 3(a). 1H-NMR Spectrum of β-CD

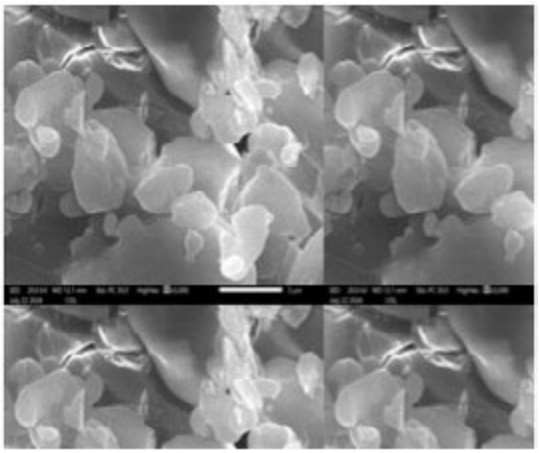

Fig.4(b). SEM analysis β-CD

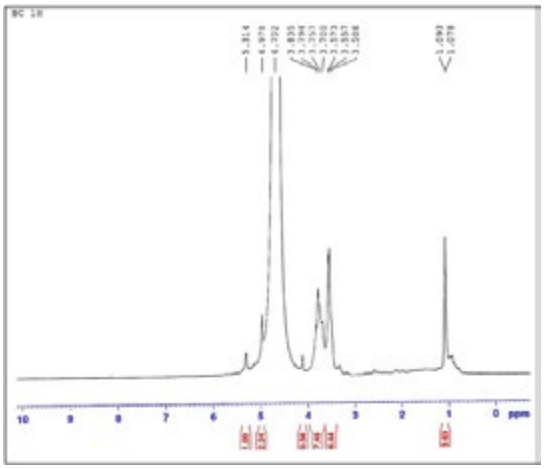

Fig. 3(b). 1H-NMR Spectrum of BCP:β-CD Inclusion complex

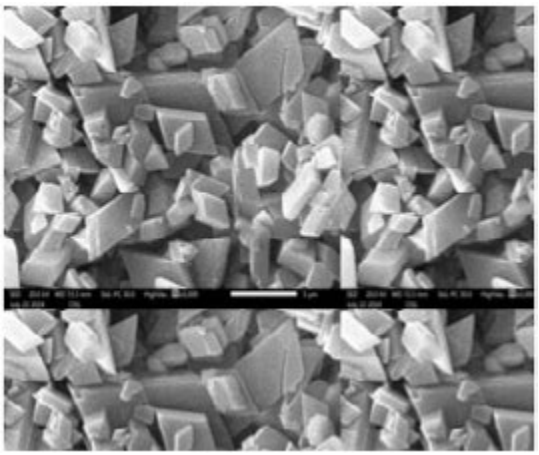

Fig. 4(c). SEM analysis BCP:β-CD

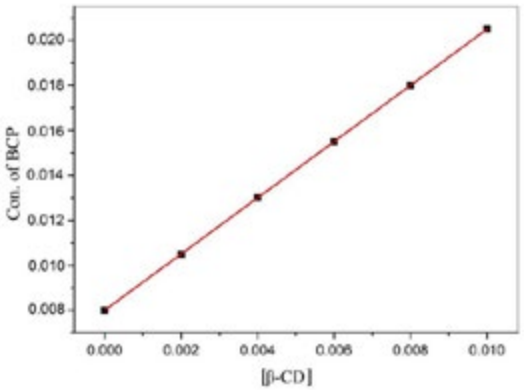

Fig. 5. Phase Solubility of BCP with β-CD

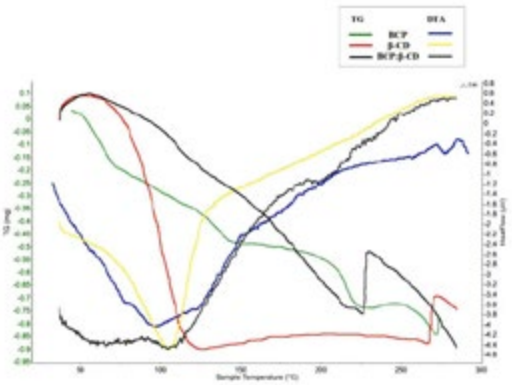

Fig. 6. Simultaneous TG-DTA Analysis of BCP, β-CD & BCP:β-CD

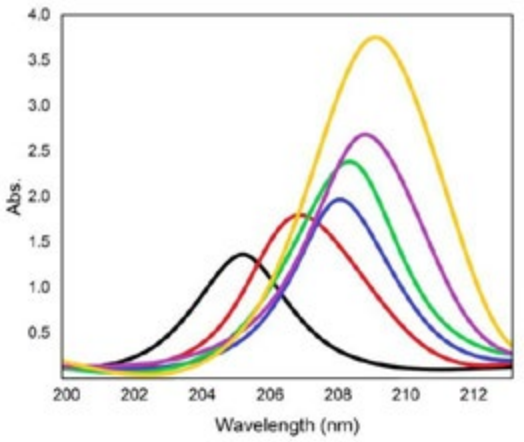

Fig. 7. Absorption of BCP with β-CD at different concentration

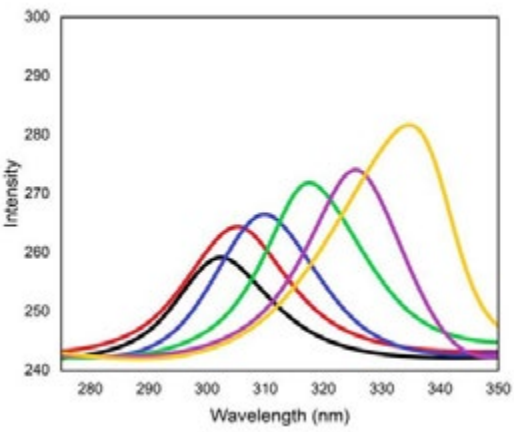

Fig. 8. Fluorescence Emission of BCP with β-CD at different concentration

Thermal Analysis

The thermal analysis results are presented in Fig. 6. The increased thermal stability of the inclusion complex compared to free BCP and βCD confirms the successful formation of a stable complex. Changes in DTA peak patterns and a shift in the degradation temperature indicate effective interaction between BCP and the β-CD cavity, providing enhanced protection to the guest molecule. Additionally, the reduced weight loss of the complex at lower temperatures suggests a decrease in BCP volatility, further supporting the efficiency of encapsulation.

Absorption study of liquid inclusion complexes

UV-Vis spectroscopy was used to examine the interaction between BCP and ββ-CD at various ββ-CD concentrations. The absorbance rises from 1.417 to 3.762, indicating improved solubility, as seen in Table 2 and Fig. 7. The formation of the BCP:ββ-CD inclusion complex is confirmed by the change in the maximum absorption wavelength ($\lambda\beta_{max}$) of BCP from 205 nm to 209 nm with increasing βCD concentration. This change indicates that the host-guest relationship is steady and that BCP has been successfully encapsulated within the β-CD cavity.

Fluorescence study of liquid inclusion complexes

The fluorescence study of BCP with varying β**-CD** concentrations is presented in Table 3 **and Fig. 8**. A **red shift** in emission wavelength from 300.8 nm to 334 nm is observed with increasing β-CD

Fig. 9. 3D structure of (a) BCP, (b) β-CD, (c) BCP docked with β-CD

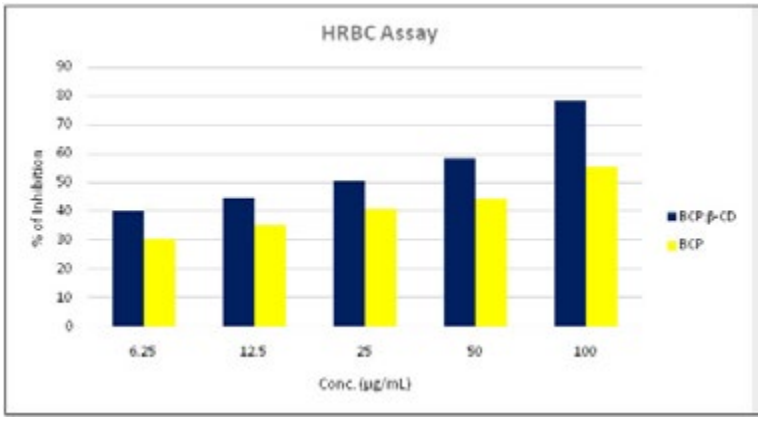

Fig. 10. Anti-Inflammatory Potential of BCP, BCP:β-CD

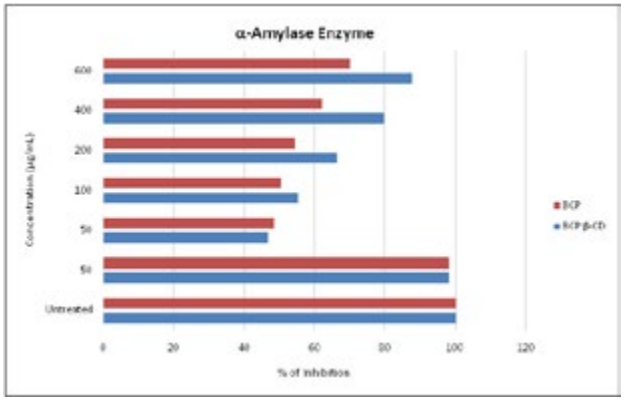

Fig. 11. Comparison of α-Amylase Inhibition

concentration, indicating a progressive interaction. The increase in **fluorescence intensity** further confirms the formation of the **BCP:β-CD inclusion complex**, suggesting successful encapsulation of BCP within the β-CD cavity. This shift towards a longer wavelength supports the stabilization of BCP in a more hydrophobic environment provided by β-CD.

The 3D molecular docking structure of BCP with β-CD is presented in Fig. 9(c), while Table 4 summarizes the binding affinity and

RMSD values. Among the docking modes, Mode 1 exhibited the lowest binding affinity of -4.952 kcal/mol and an RMSD of 0, indicating the most stable and energetically favorable inclusion complex. In this mode, BCP is deeply embedded within the hydrophobic cavity of β-CD, forming a range of stabilizing interactions. Hydrophobic interactions between the non-polar regions of BCP and the inner cavity of β-CD play a dominant role in stabilizing the complex. Additionally, **van der Waals forces** contribute to the tight fit and complementarity between the host and guest molecules. A hydrogen **bond** was observed between the hydroxyl group at the rim of ββ-CD and a polar moiety of BCP, further enhancing binding stability. These specific molecular interactions, beyond the overall binding affinity, collectively support the successful formation of a robust inclusion complex between BCP and β-CD.

Anti-inflammatory Potential

Fig.10 illustrate the percentage inhibition of heat-induced hemolysis at varying concentrations. Among the samples, BCP:ββ-CD displayed the most significant membrane stabilization effect. At 100 µg/mL, BCP showed a maximum inhibition of 78%, while the control exhibited only 55%

BCP: β -CD complex IC_{50} (26 µg/ml) value, indicating the highest anti-inflammatory potency. BCP showed IC_{50} of 75 µg/ml. These findings confirm the superior anti-inflammatory activity of the BCP:β β-CD inclusion complex.

Anti Diabetic Activity

The Fig.11 shows the βamylase inhibitory activity of BCP and BCP:ββ-CD at concentrations from 50 to 600 µg/mL. Table 5 shows that the BCP-β β-CD consistently exhibited higher % inhibition than free BCP at all concentrations. At 600 µg/mL, BCP β-CD reached 87.56% inhibition, while BCP showed 70%. The enhanced activity of the inclusion complex is due to improved solubility and interaction with the enzyme, supported by its lower IC_{50} (31.35 µg/mL) compared to BCP (90 µg/mL). confirming that the inclusion complex significantly improves antidiabetic potential through stronger α-amylase inhibition.

CONCLUSION

This study provides a comprehensive demonstration of the successful encapsulation of BCP, isolated from *Aegle marmelos* leaves, within β-cyclodextrin (β-CD) to form a stable inclusion complex. The formation and structural integrity of the complex were confirmed through multiple spectroscopic techniques including UV-Vis, fluorescence, FT-IR, and ^{1}H-NMR analyses. Phase solubility studies revealed a notable improvement in the aqueous solubility of BCP in the presence of β-CD at varying concentrations. Thermal analysis further supported the formation of the inclusion complex, showing enhanced thermal stability compared to free BCP. Molecular docking studies using AutoDock Vina indicated a strong and stable interaction between BCP and β-CD, as evidenced by favorable binding affinity and interaction profiles. The inclusion complex (BCP:β-CD) also demonstrated superior anti-inflammatory and anti-diabetic activities compared to free BCP, confirming that encapsulation enhances the therapeutic potential of the compound. Overall, this study underscores the potential of β-CD as an effective carrier to improve the solubility, stability, and bioavailability of BCP, offering promising implications for both pharmaceutical and industrial applications. **I**n the future, in vivo studies, formulation development, and toxicological assessments can **help validate** the therapeutic potential of the BCP–β CD complex and support its industrial applications.

ACKNOWLEDGEMENT

The authors gratefully acknowledge the support of the respective institutions for their instrumental support.

Conflict of Interest

The authors have no conflicts of interest to declare.

REFERENCES

1. Rajasekaran, C.; Meignanam, E.; Premkumar, N.; Kalaivani, T.; Siva, R.; Vijayakumar, V.; Ramya, S.; Jayakumararaj, R. *Ethnobotanical Leaflets*, **2008**, *12*, 1124-1128.
2. Arvind Kumar Shakya. *International Journal of Herbal Medicine*, **2016**, *4(4),* 59-64.
3. Umadevi, Kumba; Janarthanan; Vanitha; Varadharajan; Vijayalakshmi, Krishnamurthy.

World Journal of Pharmaceutical research, **2012**, *1(3),* 813-837.
4. Suresh, Janadri; Ranjith, Kumar, R.; Manjunatha, P. M.; Uday, Raj, Sharma; Surendra, Vada; Madhu, M. V.; Preeti, P. Angadi. *Defence Life Science Journal*, **2025**, *10(1),* 65-71.
5. Hua, Liu; Guang, Yanga; Yuanjun, Tanga; Di, Cao; Tian, Qi; Yunpeng, Qi.; Guorong, Fan. *International Journal of Pharmaceutics,* **2013**, 1-7.
6. Bakır, B.; Him, A.; Ozbek, H.; Duz, E.; Tutuncu, M. *International Journal of Essential Oil Therapeutics,* **2008**, *2*, 41-44.
7. Patil, J. S.; Kadam, D. V.; Marapur, S. C.; Kamalapur, M. V. *International Journal of Pharmaceutical Sciences Review and Research,* **2010**, *2(2),* 29–34.
8. Romina, L. Abarca.; Francisco, J. Rodríguez.; Abel, Guarda; Maria, J. Galotto; Julio, E. Bruna. *Food Chemistry,* **2016**, *196*, 968-975.
9. Martin, E. M.; Del, Valle. *Process Biochemistry,* **2004**, *39***(9)**, 1033–1046.
10. Soumyadeep, Sain; Pravin, K.; Naoghare, S.; Saravana, Devi; Atul, Daiwile, K.; Krishnamurthi, P. Arrigo; Chakrabarti, T. *Anti-Inflammatory & Anti-Allergy Agents in Medicinal Chemistry,* **2014**, *13(1),* 45-55.
11. Benesi, H. A.; Hildebrand, J. H. *Journal of the American Chemical Society*, **1949**, *71(8),* 2703-2707.
12. Higuchi, T.;Connors, K. A. *Advances in chemical Instrumentation*, **1965**, *4*, 212-217.
13. Ming, Chen; Guowang, Diao; Enren Zhan. *Chemosphere,* **2006**, *63*, 522–529.
14. Eberhardt, J.; Santos-Martins, D.; Tillack, A. F.; Forli, S. *Journal of Chemical Information and Modeling*, **2021**, *61*(8), 3891–3898.
15. Trott, O.; Olson, A. J.; *Journal of Computational Chemistry*, **2010**, *31(2),*455–461.
16. Heidari, R.; Zareae, S.; Heidarizadeh, M.; *Pakistan Journal of Nutrition,* **2005**,*4(2),* 101–105.
17. Shai, L. J.; Masoko, P.; Mokgotho, M. P.; Magano, S. R.; Mogale, M. A.; Boaduo, N.; Eloff, J. N.; *South African Journal of Botany,* **2010,** *76*, 465–470.
18. Sakat, S.; Juvekar, A. R.; Gambhire, M. N. *International Journal of Pharmacy and Pharmaceutical Sciences,* **2010**, *2*, 146–155.
19. Shinde, U. A.; Kulkarni, K. R.; Phadke, A. S.; Nair, A. M.; Dikshit, V.; Mungantiwar, J.; Saraf, M. N. *Indian Journal of Experimental Biology*, **1999**, *37*, 258–261.